Origins: From the Protosun to the First Steps of Life
Proceedings IAU Symposium No. 345, 2018
B. G. Elmegreen, L. Viktor Tóth & M. Güdel, eds.

doi:10.1017/S1743921318008311

The first 200 kyr of the Solar System: making the planetary material diversity

Francesco C. Pignatale[1,2], Sébastien Charnoz[2], Marc Chaussidon[2] and Emmanuel Jacquet[1]

[1]Muséum national d'Histoire naturelle, UMR 7590, CP52, 57 rue Cuvier, 75005, Paris, France
email: pignatale@ipgp.fr

[2]Institut de Physique du Globe de Paris (IPGP)
1 rue Jussieu, 75005, Paris, France

Abstract. Chondrites are made of a mixture of solids formed at high and low temperatures. This heterogeneity was thought to be produced by large scale transport processes in the Sun's isolated accretion disk. However, mounting evidences suggest that refractory inclusions in chondrites were produced together with the disk formation.

We present numerical simulations of the formation and transport of rocky materials during the collapse of the Solar Nebula's parent cloud and the consequent disk assembling.

We find that the interplay between the cloud collapse, the dynamics of gas and dust and thermal processing of different species in the disk, results in a local mixing of solids with different thermal histories. Our simulations return an heterogeneous distribution of refractory material with higher concentration in the outer disk. This refractory material has a short formation timescales, during the first tens of kyr of the Sun (class 0-I). Our results open new frontiers into the origin of the compositional diversity of chondrites.

Keywords. solar system: formation, meteors, meteoroids, stars: formation, (stars:) planetary systems: protoplanetary disks

1. Introduction

Chondrites are undifferentiated meteorites formed within the first 4 Myr of the Solar System history (with the age determined by the oldest compoments, Ca-Al-rich inclusions, CAIs). They are a mixture of components formed at high and low temperature (see Scott & Krot (2003)). This peculiar mixture is one important ingredient in the composition of terrestrial planets and its formation processes are still unknown. A paradox is that carbonaceous chondrites, which are thought to have accreted in the outer Solar System at temperatures lower than 150 K (see Warren (2011)) are enriched in CAIs (formed at $T > 1600$ K) and close to the Sun) when compared with other chondrites (see Scott & Krot (2003)).

The chemical composition of CAIs links them with condensate precursors (see Richter *et al.* (2006)) formed during a short interval of time, around $t \sim 160$ kyr (see Connelly *et al.* (2012)). This timescale is shorter than the formation time of a protoplanetary disk from its parent collapsing cloud, and suggests that the formation of the first solids occurred simultaneously with the building of our Solar Nebula. This is supported by observational evidence of young sellar objects that show crystalline dust in their infrared spectra as soon as the star begins to form, as described by Williams & Cieza (2011) and Chiang *et al.* (2012).

In order to understand the formation and accretion processes of chondrites components, we developed a 1D simulation to track the thermal evolution of dust with

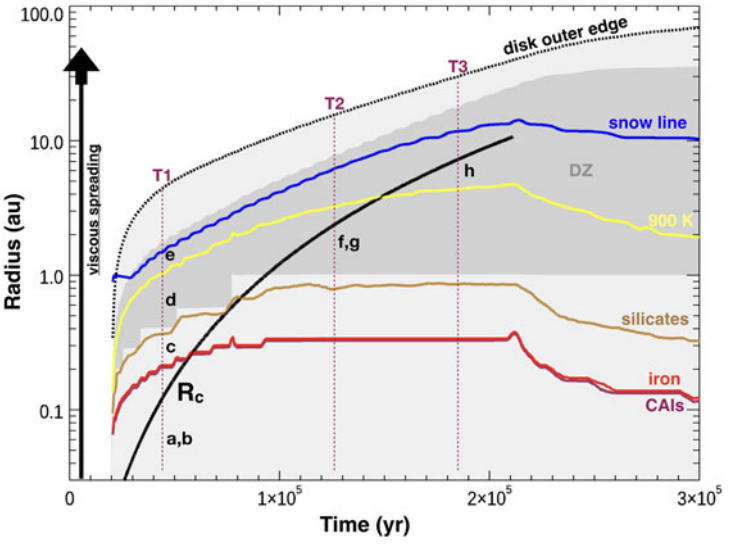

Figure 1. Time evolution of the centrifugal radius (black solid line) and the locations of disk outer edge, different condensation fronts, and dead zone (dark grey). Figure adapted from Pignatale *et al.* (2018) and reproduced by permission of the AAS.

different composition during the collapse of the parent cloud and the formation of the protoplanetary disk.

2. Method

We model a classical alpha-disk starting from Hueso & Guillot (2005) that considers a collapsing cloud with radiative and viscous heating. Our 1D disk is described by a logarithmic grid (100 cells, between 0.01 and 1000 au). We include the modellisation of a dead zone (DZ) in the form of a parameterized description. We consider a layered accretion model with a low-α midplane and high-α surface layers, dust transport through advection and diffusion, and growth/fragmentation. We also include gravitational instability. The opacity is calculated using an opacity table. A detailed description of the code, methods and references is reported in Pignatale *et al.* (2018) and in Charnoz *et al.* (2019).

Improving on the work of Yang & Ciesla (2012), we now include multiple chemical species allowing material condensation, sublimation and thermal processing using a simple chemical model. We then track the formation and transport in the disk of gaseous species and different solid species with their vaporisation temperatures: (i) condensed refractory phases, that we consider potential precursors of CAIs, (ii) condensed metal (iii) condensed silicates, (iv) thermally processed and unprocessed silicates, (v) thermally processed and unprocessed iron, (vi) water ice, and (vii) CO ice. The main gas species is molecular hydrogen.

3. Results

Figure 1 shows the time evolution of the centrifugal radius ($R_c(t)$), the locations of disk outer edge, different condensation fronts, and dead zone (dark grey). As the dust is injected into the forming disk, its composition and thermal structure change because of heating of species with different vaporisation temperatures. Because of angular momentum constraints, R_c(t) is initially close to the forming Sun fed from the parent cloud's innermost regions (see Kimura *et al.* (2016)). Then R_c(t) increases with time due to the arrival of originally more distant cloud materials with higher specific angular momentum.

https://doi.org/10.1017/S1743921318008311 Published online by Cambridge University Press

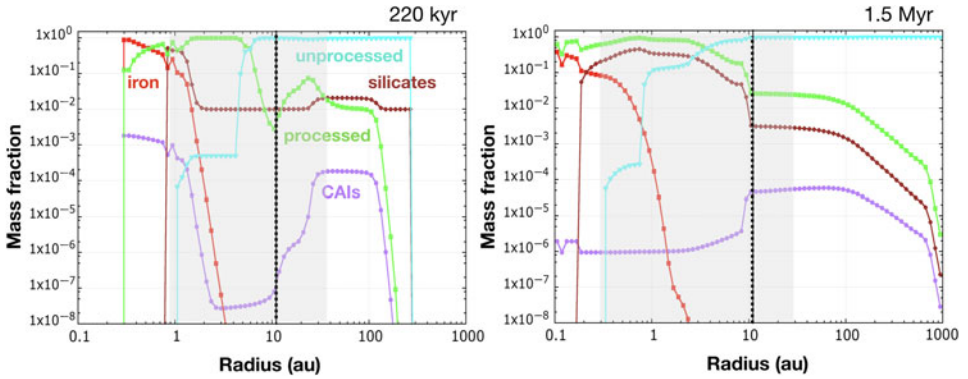

Figure 2. Mass fraction of various types of rocky material in the disk as a function of radius and time. The different types of solids considered are CAIs (purple), metallic iron (red), condensed silicates (brown), all processed dust (green), all unprocessed dust (cyan). Figure adapted from Pignatale *et al.* (2018) and reproduced by permission of the AAS.

At $t \sim 50$ kyr (T1), $R_c(t)$ is within the condensation fronts of the most refractory species (CAIs and iron) so that all the dust injected with the gas (a) is vaporised (b). At the same time, further out in the disk, condensation of CAIs and iron (c) silicates (d) takes place from a gas which is spreading outwards. Iron condensed and transported with the spreading gas can be processed further out (e). At $t \sim 120$ kyr (T2), R_c(t) has reached a region in the disk where the temperature is below 1500 K. Presolar refractory material and silicates can be injected into the disk without being vaporised (f) but they can experience thermal processing (g). At $t \sim 180$ kyr (T3), parent cloud material is injected in the disk likely retaining its primordial texture as the temperature is too low for thermal processing (h).

Figure 2 shows two time snapshots of the mass fraction of the considered rocky material as a function of the distance from the central star. The light grey zone shows the extension of the dead zone. The black dotted line shows the location of the centrifugal radius $R_c(t)$. It can be seen that, at the end of collapse, $t \sim 220$ kyr, $R_c(t)$ penetrates the DZ where dust and gas can be stored because of very low turbulence. This lowers dramatically the concentration of refractory condensates within the DZ. This leads to a DZ poor in refractory condensates and a CAIs-enriched outer disk beyond the DZ. This dust distribution will qualitatively preserve its heterogeneity over the lifetime of the disk ($t \sim 1.5$ Myr). Inward the DZ inner edge ($R < 0.3$ AU), the disk becomes CAIs-poor because of strong accretion of gas that removes solids.

The resulting distribution for the various dust components in the disk ($t \sim 1.5$ Myr) shows an overall agreement with the composition of enstatite, ordinary, carbonaceous chondrites as defined by their fractions of CAIs, metal, chondrules and matrix (see Scott & Krot (2003)). We consider the unprocessed dust as a proxy for the fine-grained matrix containing different kinds of circumstellar grains which are likely surviving interstellar grains. In the inner disk region ($1 < R < 10$ au), dust is dominated by disk-born silicates and iron (processed or condensed) and poor in CAIs and pristine interstellar dust. This reminds of (matrix-poor, chondrule-rich) non-carbonaceous chondrites (ordinary chondrites and enstatite). At larger distances from the central star, the dust is dominated by unprocessed dust that was injected late when $R_c(t) > 5$ au, processed dust and condensed silicates. This region, although beyond the snow-line and having water ice-bearing dust, has the highest fraction of CAIs. This reminds the carbonaceous chondrites.

https://doi.org/10.1017/S1743921318008311 Published online by Cambridge University Press

Our simulations also show that the production of CAIs occurs within the first $t \sim 80$ kyr (see Pignatale *et al.* (2018)). This in very good agreement with Pb–Pb and ^{26}Al–^{26}Mg chronologies of CAIs as shown by Connelly *et al.* (2012) and Mishra & Chaussidon (2014). This is a very short interval of time, when interstellar dust is injected in the forming disk at temperatures high enough to be fully evaporated (i.e. when $R_c(t)$ is inward the condensation radius of CAIs, see Fig.1), so that upon spreading outward, the gas re-condense into CAIs.

4. Conclusions

We investigated the effects of coupling thermal processing and transport of dust during the collapse of a parent cloud and the consequent disk formation. This naturally results in a local mixing of materials with different thermal histories. Our resulting dust radial distribution shows qualitative agreement with enstatite, ordinary and carbonaceous chondrites. Our model reconciles with the overabundance of refractory materials at large disk radii and their formation timescales, placing the time 0 of the Solar System during the class 0 to I of the Sun's formation.

References

Charnoz, S., Pignatale, F.C., Hyodo, R., *et al.* 2019, *A&A*, Astronomy and Astrophysics, 627, A50.
Chiang, H.-F., Looney, L. W., & Tobin, J. J. 2012, *ApJ*, The Astrophysical Journal, 756, 168
Connelly, J. N., Bizzarro, M., Krot, A. N., *et al.* 2012, Science, 338, 651
Hueso, R., & Guillot, T. 2005, *A&A*, Astronomy and Astrophysics, 442, 703
Kimura, S. S., Kunitomo, M., & Takahashi, S. Z. 2016, *MNRAS*, Monthly Notices of the Royal Astronomical Society, 461, 2257
Mishra, R. K., & Chaussidon, M. 2014, Earth and Planetary Science Letters, 390, 318
Pignatale, F. C., Charnoz, S., Chaussidon, M., & Jacquet, E. 2018, *ApJL*, 867, L23
Richter, F. M., Mendybaev, R. A., & Davis, A. M. 2006, Meteoritics and Planetary Science, 41, 83
Scott, E. R. D., & Krot, A. N. 2003, Treatise on Geochemistry, 1, 711
Yang, L., & Ciesla, F. J. 2012, Meteoritics and Planetary Science, 47, 99
Warren, P. H. 2011, Geo Cos Acta, 75, 6912
Williams, J. P., & Cieza, L. A. 2011, *ARAA* Annual Review of Astronomy and Astrophysics, 49, 67

Discussion

Lissauer: What causes the differences you find between the distribution of condensed iron and silicates which have similar condensation temperature in standard model?

Pignatale: This depends on the steepness of the resulting temperature gradient as a function of the distance from the central star. And also on the fiducial condensation temperatures chosen for the selected species.

Linsky: Thank you for the excellent presentation of a thermal steady state simulation. However star flares and interaction between the stellar and disk magnetic field can produce heat, and episodic UV and X-ray emission that can lead to different results from your calculations.

Pignatale: That is right. However this will not affect how the material will distribute during the disk building, and temperature in the inner disk is dominated by the dissipation of turbulence. Nevertheless, the events you mentioned can actually make the production, alteration and transport of refractory material easier.

https://doi.org/10.1017/S1743921318008311 Published online by Cambridge University Press